12-2-2019

Thermodynamic Model of CO2 Deposition in Cold Climates

Sandra K. S. Boetcher
Embry-Riddle Aeronautical University, boetches@erau.edu

Ted von Hippel
Embry-Riddle Aeronautical University, vonhippt@erau.edu

Matthew J. Traum
University of Florida, mtraum@ufl.edu

Scholarly Commons Citation

Boetcher, S.K.S., Traum, M.J. & von Hippel, T. Thermodynamic Model of CO2 Deposition in Cold Climates. Climatic Change 158, 517–530 (2020). https://doi.org/10.1007/s10584-019-02587-3

Climatic Change (2020) 158:517–530
https://doi.org/10.1007/s10584-019-02587-3

Thermodynamic Model of CO_2 Deposition in Cold Climates

Sandra K. S. Boetcher[1] · Matthew J. Traum[2] · Ted von Hippel[3]

Received: 10 May 2019 / Accepted: 22 October 2019 / Published online: 2 December 2019

Abstract

A thermodynamic model, borrowing ideas from psychrometric principles, of a cryogenic direct-air CO_2-capture system utilizing a precooler is used to estimate the optimal CO_2 removal fraction to minimize energy input per tonne of CO_2. Energy costs to operate the system scale almost linearly with the temperature drop between the ingested air and the cryogenic desublimation temperature of CO_2, driving siting to the coldest accessible locations. System performance in three Arctic/Antarctic regions where the proposed system can potentially be located is analyzed. Colder ambient temperatures provide colder system input air temperature yielding lower CO_2 removal energy requirements. A case is also presented using direct-sky radiative cooling to feed colder-than-ambient air into the system. Removing greater fractions of the ingested CO_2 lowers the CO_2 desublimation temperature, thereby demanding greater energy input for air cooling. It therefore is disadvantageous to remove all CO_2 from the processed air, and the optimal mass fraction of CO_2 desublimated under this scheme is found to be ~0.8-0.9. In addition, a variety of precooler effectiveness (ε) values are evaluated. Increasing effectiveness reduces the required system power input. However, beyond $\varepsilon = 0.7$, at certain higher values of desublimated CO_2 mass fraction, the CO_2 begins to solidify inside the precooler before reaching the cryocooler. This phenomenon fouls the precooler, negating its effectiveness. Further system efficiencies can be realized via a precooler designed to capture solidified CO_2 and eliminate fouling.

Keywords CO_2 desublimation · thermodynamics · cryogenics · Arctic/Antarctica

✉ Sandra K. S. Boetcher
sandra.boetcher@erau.edu

Matthew J. Traum
mtraum@ufl.edu

Ted von Hippel
ted.vonhippel@erau.edu

Extended author information available on the last page of the article

1 Introduction

The IPCC's most recent report (IPCC 2018) highlighted that humanity will overshoot safe levels for anthropogenic greenhouse gases, stating: "All pathways that limit global warming to 1.5 °C with limited or no overshoot project the use of carbon dioxide removal (CDR) on the order of 100-1000 $GtCO_2$[1] over the 21st century." This result, also derived earlier (Hansen et al. 2008), means that capturing CO_2 at power plants or other sources, while necessary, will not be sufficient, and therefore direct air capture (DAC) of CO_2 will be required, despite the fact that it is energetically more costly than CO_2 capture at the source (Baxter et al. 2009). This report also noted that "The energy requirements and economic costs of direct air carbon capture and storage ... remain high," yet with only medium evidence and medium agreement on that statement. Anthropogenic atmospheric CO_2 plays the largest role among greenhouse gasses in modifying Earth's climate, and several research groups are working on CO_2 removal directly from the air. Among these approaches, adsorption, absorption, and membrane separation still require considerable research to develop and scale the technologies. Lack of 1) clear technology maturity, 2) viable energy requirement estimates, and 3) cost estimates to implement these direct carbon removal approaches necessitate more research in DAC (see Keith et al. 2006; Lackner et al. 2012) of excess greenhouse gases. By contrast, the components in developing a cryogenic CO_2 DAC system are well understood, making the potential of a rapid scale-up of this technology more straightforward than the other methods previously mentioned.

This paper explores a practical direct-air greenhouse-gas capture and removal technique that can be implemented by scaling up existing cryogenic refrigeration technologies. It does not rely on speculative future breakthroughs. Desublimation (vapor-to-solid) phase change of pure CO_2 at 1 atm pressure occurs at 194.65 K (-78.5 °C). However, for effluent that is not pure CO_2, partial pressure below 1 atm lowers the desublimation temperature, necessitating additional cooling for CO_2 solidification and extraction. Nonetheless, in atmospheric air, the CO_2 desublimation temperature is higher than phase-change temperatures for any other gaseous component except water (Agee et al. 2013), even at fractional CO_2 concentrations from 1 - 400 ppm. This serendipitous thermodynamic attribute of air enables CO_2 gas removal via direct cryogenic desublimation, but it also introduces an optimization problem.

The current study builds upon recent ideas and thermodynamic analyses (Agee et al. 2013; Agee and Orton 2016; von Hippel 2018), which studied cooling vast volumes of air to the point where CO_2 desublimates from the atmosphere. This approach capitalizes on frigid ambient polar temperatures to provide a reservoir of cold atmospheric air requiring less cooling than temperate air. Units sited in Arctic and Antarctic regions draw in atmospheric air, further cooling it to CO_2 desublimation temperatures for greenhouse gas removal. The scrubbed air is then returned to the atmosphere. If deployed at large scale over 50-100 years, this technique has the potential to reduce atmospheric CO_2 to levels low enough to mitigate anthropogenic global climate change. When optimized, the estimated energy input of this approach is ~50 GJ/tonne CO_2 (see Section 5).

In the current paper, these thermodynamic studies are tested and extended by borrowing from the tools of psychrometrics, the thermodynamic analysis of air/water-vapor mixtures. These tools are broadly applicable to the behavior of mixed fluids, including at or near phase transitions. Specifically, psychrometrics are applied to air/CO_2 mixtures as dry air is cooled from the ambient

[1] one Gt = 10^9 metric tons, written as tonnes

temperature to below its desublimation point. The consistency of these new calculations is compared with prior work and their implications for real-world systems are discussed.

The proposed system is composed of two key components: a cryocooler and a precooler. A cryocooler chills air to CO_2 desublimation temperatures by removing heat via cryogenic refrigeration. Practical units that exist today can maintain CO_2 desublimation temperature operating with efficiencies 15% of the theoretical Carnot coefficient of performance (COP). Work into the cryocooler is the principle energy input required to achieve the ~50 GJ/tonne CO_2 removal rate. Since the whole volume of processed air must be reduced to the CO_2 desublimation temperature to extract the greenhouse gas, it is advantageous to recapture that cold using a precooler. This device is a heat exchanger that uses the cooling capacity of the cold air leaving the cryocooler to chill ambient air entering the desublimator. The precooler consumes no energy other than requiring a fan to overcome a small amount of backpressure, and it induces an order-of-magnitude reduction in the cryocooler power input needed to maintain the CO_2 desublimation temperature from ~500 to ~50 GJ/tonne CO_2. The precooler, therefore, is a critical component of the direct-air CO_2 desublimation system to improve efficiency. The relative merits of an additional component, a radiative cooler, are also tested. Radiative cooling takes advantage of the fact that the night sky has a nonthermal spectrum that can be matched to the optical emissivity properties of a radiator to achieve temperatures below the ambient temperature (see Section 2.3).

2 Thermodynamic modeling of CO_2 deposition chamber

Psychrometrics is the science of thermodynamic behavior of air/water-vapor mixtures. The study of psychrometrics usually pertains to heating, ventilating, and air-conditioning (HVAC) and human thermal comfort inside of buildings. Heating and cooling loads can be calculated via energy balances utilizing thermodynamic principles behind air/water-vapor mixtures.

One measure of human thermal comfort is determined by the humidity, which is the amount of water vapor in the air. If there is too much water vapor in the air, the air will need to be dehumidified to restore human comfort. One way to dehumidify air is by cooling moist air below its dew point temperature so that condensation of water occurs. The condensed water can then be easily removed.

Except for water vapor (which is easily condensed out at very low temperatures), CO_2 is the fourth most abundant atmospheric gas, and it possesses the highest phase-change temperature (-78.5 °C) at atmospheric pressure, becoming solid dry ice. The proposed air CO_2 removal system capitalizes on this thermodynamic property of the greenhouse gas to remove it from air at relatively high temperature compared to liquification temperatures of air's other major components at atmospheric pressure: nitrogen (-195.8 °C), oxygen (-183.0 °C), and argon (-185.8 °C).

The idea underpinning the present study is to apply principles of psychrometrics, but replace water vapor in air/water-vapor mixtures with CO_2 to perform thermodynamic analysis of CO_2 deposition in cold climates.

2.1 Governing Equations

Borrowing ideas from psychrometrics, the total enthalpy, H, for an air/ CO_2 mixture is proposed as

$$H = H_a + H_{CO_2} = m_a h_a + m_{CO_2} h_{CO_2} \tag{1}$$

Here, H_a is the total enthalpy of the air, H_{CO_2} is the total enthalpy of the CO_2, m_a and m_{CO_2} are the masses of the air and CO_2, respectively, and h_a and h_{CO_2} are the specific enthalpy of the air and CO_2.

The specific enthalpy of the mixture, h, is the total enthalpy of the air/CO_2 per unit mass of the air

$$h \equiv \frac{H}{m_a} = h_a + \frac{m_{CO_2}}{m_a} h_{CO_2} \tag{2}$$

A thermodynamic analysis will now be performed for the CO_2 deposition chamber illustrated in Fig. 1.

The conservation of mass for the air is

$$\dot{m}_{a,1} = \dot{m}_{a,2} = \dot{m}_a \tag{3}$$

where $\dot{m}_{a,1}$ and $\dot{m}_{a,2}$ are the mass flow rates of air at states 1 and 2 and equal to just $\dot{m}_a$.

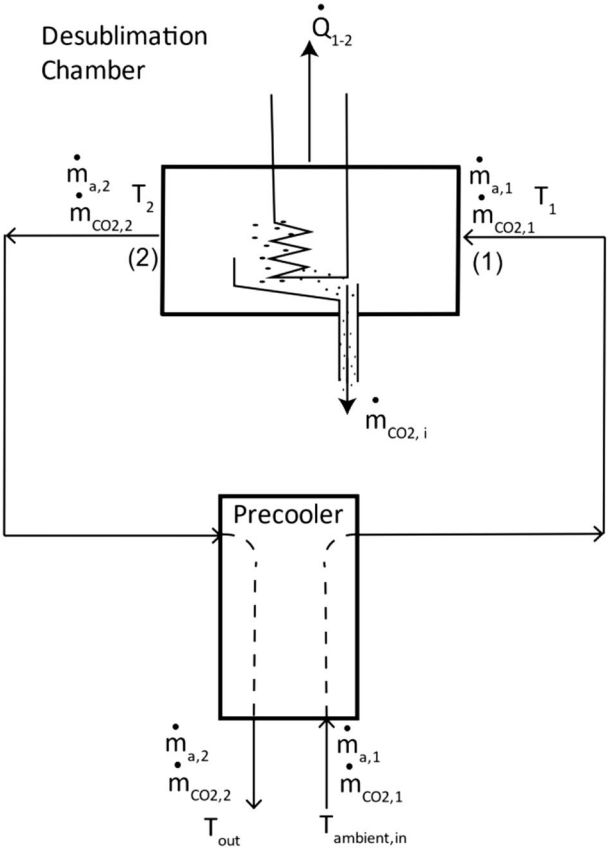

Fig. 1 Schematic diagram of the CO_2 deposition chamber with added precooler

The conservation of mass for the CO_2 is

$$\dot{m}_{CO_2,1} = \dot{m}_{CO_2,2} + \dot{m}_{CO_2,i} \tag{4}$$

Here, $\dot{m}_{CO_2,1}$ and $\dot{m}_{CO_2,2}$ are the mass flow rates of the CO_2 at states 1 and 2, and $\dot{m}_{CO_2,i}$ is the mass flow rate of the CO_2 desublimated from the atmosphere. The amount of CO_2 desublimated from the atmosphere is defined by the mass fraction ω where

$$\omega = \frac{\dot{m}_{CO_2,i}}{\dot{m}_{CO_2,1}} \tag{5}$$

Therefore,

$$\dot{m}_{CO_2,i} = \omega \dot{m}_{CO_2,1} \tag{6}$$

and

$$\dot{m}_{CO_2,2} = (1-\omega)\dot{m}_{CO_2,1} \tag{7}$$

The steady-state energy balance for the open system is

$$\dot{Q}_{1-2} + \dot{m}_{a,1}h_1 = \dot{m}_{a,2}h_2 + \dot{m}_{CO_2,i}h_{CO_2,i} \tag{8}$$

Here, $\dot{Q}_{1-2}$ is the heat transfer rate required to desublimate mass fraction, ω, of the CO_2. The enthalpies h_1 and h_2 are the total specific enthalpies at states 1 and 2, respectively. The enthalpy of the saturated solid CO_2 exiting the chamber is $h_{CO_2,i}$. Dividing this equation by the air mass flowrate $\dot{m}_a$ (see Eq. 3) and rearranging yields

$$\frac{Q_{1-2}}{m_a} = \frac{\dot{Q}_{1-2}}{\dot{m}_a} = h_2 - h_1 + \frac{\dot{m}_{CO_2,i}}{\dot{m}_a}h_{CO_2,i} \tag{9}$$

where $Q_{1-2}/m_a = \dot{Q}_{1-2}/\dot{m}_a$ is the thermal energy required to desublimate the CO_2 per unit mass air and $\dot{m}_{CO_2,i}/\dot{m}_a$ is the mass fraction of CO_2 desublimated with respect to a unit mass of air.

To convert heat removal required per mass of air to per mass of CO_2 desublimated

$$\frac{Q_{1-2}}{m_{CO_2,i}} = \frac{Q_{1-2}}{m_a}\frac{m_a}{m_{CO_2,i}} \tag{10}$$

2.2 Thermal properties

REFPROP, a program developed by the National Institute of Standards and Technology (NIST) to calculate thermodynamic properties, was used (Lemmon et al. 2018). Air data (0.7812 N_2, 0.2096 O_2, and 0.0092 Ar on a molar basis) were calculated from equations of state developed by Lemmon et al. (2000). The CO_2 equation of state was developed by Span and Wagner (1996).

Although a concentration of 100% CO_2 desublimates at -78.5 °C at atmospheric pressure, when the concentration of CO_2 is less than 100%, a lower temperature is required. In fact, the lower the concentration of CO_2, the lower the temperature needed to desublimate. The vapor pressure of CO_2 in the atmosphere is needed to calculate the desublimation temperature. The

concentration of CO_2 in the environment is assumed to be 405 ppmv which is equal to a mole fraction of $x_{CO_2,1} = 0.000405$ at the inlet of the deposition chamber (Fig. 1, state 1). The partial pressure of the CO_2 at state 1 is calculated by

$$P_{CO_2,1} = x_{CO_2,1} P \tag{11}$$

where P is the total atmospheric pressure. Assuming P = 1 atm and $P_{CO_2,1}$ = 0.000405 atm, this corresponds to a desublimation temperature of T_i = -141.66 °C. Although the CO_2 starts to desublimate at a temperature of -141.66 °C at that partial pressure, as the CO_2 continues to desublimate, the partial pressure decreases and the desublimation temperature also decreases. The temperature used as the desublimation temperature T_2 was taken to be the desublimation temperature of the partial pressure of CO_2 in the atmosphere after an amount of mass fraction ω has desublimated (see Table 1). For example, if a mass fraction ω = 0.4 is assumed to have desublimated, then a mass fraction of ω = 0.6 of CO_2 is left at state 2 in Fig. 1. The partial pressure of the CO_2 at state 2 was used to calculate the desublimation temperature.

The O_2 in the atmosphere begins to liquefy at -183 °C. As seen in Table 1, a temperature of -161.96 °C is required to remove 99% of the CO_2 by mass, so virtually all of the CO_2 can be removed from the atmosphere before the next component, O_2 begins to liquefy.

The latent heat of sublimation h_{ig} of the CO_2 was determined by using the Clausius-Clapeyron Equation (Moran et al. 2018)

$$ln\frac{P_{vap,2}}{P_{vap,1}} = \frac{h_{ig}}{R}\left(\frac{1}{T_1} - \frac{1}{T_2}\right) \tag{12}$$

where P_{vap} is the vapor pressure, T is the temperature in absolute units, and R is the ideal gas constant.

2.3 Thermodynamic analysis

Four very cold ambient environments were considered: Snag, Yukon (-20 °C), Oymyakon, Russia (-40 °C), and Vostok Station, Antarctica (-65 and -90 °C) with the coldest temperature including radiative cooling to the Antarctic night sky. Cooling from radiative coupling with the night sky takes advantage of the nonthermal sky

Table 1 Temperature required to desublimate ω of CO_2

ω	T_i [°C]
0.99	-161.96
0.95	-155.69
0.90	-152.74
0.80	-149.62
0.70	-147.72
0.60	-146.33
0.50	-145.22
0.40	-144.31
0.30	-143.52
0.20	-142.83
0.10	-142.21
0	-141.66

spectrum dominated by H_2O and CO_2 emission. As an example, infrared spectra of the sky over Barrow, Alaska shows emission with a brightness temperature of approximately 245 K (-28 °C) between 13 and 17 μm, yet as low as 160 K (-113 °C) at other wavelengths (Marty et al. 2003; Petty 2008). The night sky spectrum over Antarctica is qualitatively similar and even colder (Walden et al. 1998). Tests at a midlatitude site (Chen et al. 2016) show that a simple blackbody thermal radiator can reach an equilibrium temperature approximately 20 °C cooler than its environment, while an advanced thermal radiator coupled to the atmospheric transparency window from 8 to 13 μm can maintain an average equilibrium temperature 37 °C cooler than its environment. In this case, 25 °C radiative cooling was chosen because such radiative cooling would not be in equilibrium, but rather would be removing heat constantly from the ambient air before it is ingested into the system. These four ambient air temperatures were set equal to $T_{ambient,\ in}$. The concentration of CO_2 in the atmosphere is assumed to be 405 ppmv in each case.

The thermodynamic analysis was conducted assuming that the mass flow rate of the air is $\dot{m}_a$ = 1 kg/s. Assuming the molecular weight of dry air to be 28.97 g/mol and the molecular weight of CO_2 to be 44.01 g/mol, the amount of CO_2 in 1 kg of air with a CO_2 concentration of 405 ppmv is 6.153×10^{-4} kg. It was also assumed that the deposition chamber heat exchanger is able to desublimate mass fraction ω of the CO_2. The value of ω was parametrically varied from 0 to 0.99.

3 Precooler heat exchanger

A precooler heat exchanger is added to harvest the leftover cooling capacity of the cold air exiting the deposition chamber to pre-cool the ambient air entering the deposition chamber. A schematic diagram is shown in Fig. 1.

3.1 Heat exchanger analysis

Typically heat exchangers comprise two working fluids, one designated the "hot" fluid and one designated the "cold" fluid. The effectiveness of a heat exchanger is defined as

$$\epsilon = \frac{\dot{Q}_{HX}}{\dot{Q}_{HX,max}} \tag{13}$$

In this equation $\dot{Q}_{HX}$ is the heat transfer rate between the hot and cold fluid. Assuming a perfectly insulated heat exchanger

$$\dot{Q}_{HX} = C_h\left(T_{h,in} - T_{h,out}\right) = C_c\left(T_{c,out} - T_{c,in}\right) \tag{14}$$

In this equation, $T_{h,\ in}$ and $T_{h,\ out}$ are the inlet and outlet temperatures of the hot fluid, and $T_{c,\ in}$ and $T_{c,\ out}$ are the inlet and outlet temperatures of the cold fluid. C_h and C_c are the capacity rates of the hot and cold fluids where the capacity rate is defined as

$$C = \dot{m} c_p \tag{15}$$

where $\dot{m}$ is the mass flow rate of the fluid stream and c_p is the specific heat capacity.

The maximum possible heat transfer between the two fluids is

$$\dot{Q}_{HX,max} = C_{min}\left(T_{h,in} - T_{c,in}\right) \tag{16}$$

where C_{min} is the capacity rate (the product of mass and specific heat capacity) of the stream with the minimum capacity rate. Therefore, one can write

$$\epsilon = \frac{\dot{Q}_{HX}}{\dot{Q}_{HX,max}} = \frac{C_h\left(T_{h,in} - T_{h,out}\right)}{C_{min}\left(T_{h,in} - T_{c,in}\right)} = \frac{C_c\left(T_{c,out} - T_{c,in}\right)}{C_{min}\left(T_{h,in} - T_{c,in}\right)} \tag{17}$$

If the effectiveness of the heat exchanger can be determined, and both inlet temperatures are known, then both outlet temperatures can be determined. The effectiveness can be determined by the type and size of heat exchanger.

3.2 Precooler analysis

The goal of the precooler is to use the cold air exiting the deposition chamber to precool the air entering the deposition chamber. If the air entering the deposition chamber is precooled, then less energy is required to cool the air down to the CO_2 desublimation temperature.

Assuming different values of the effectiveness, a new value of T_1 is determined and a new value of Q_{1-2} per unit mass air or CO_2 is calculated (Eqs. 9 and 10). In Fig. 1, $T_{ambient,\,in} = T_{h,\,in}$, $T_1 = T_{h,\,out}$, $T_2 = T_{c,\,in}$, and $T_{out} = T_{c,\,out}$. By making the following assumptions, the capacity rates in Eq. 17 are equal, $C_c = C_h$, and they will cancel. 1) The mass flow rate of air in both precooler streams are constant because the mass of extracted CO_2 from the outlet stream is tiny compared to the overall mass. 2) For purposes of the current investigation, the specific heat capacity of both streams can be taken as constant.

Five different values of ϵ were analyzed. In order to explore the maximum limit in value of the precooler, effectiveness values of 0.9 and 0.95 were analyzed. Designing a heat exchanger to perform at those high epsilon values may not be worth the cost; therefore, other values of ϵ were explored. The value $\epsilon = 0.7$ is used for a very well-functioning heat exchanger, $\epsilon = 0.4$ for a moderately functioning heat exchanger, and $\epsilon = 0.1$ for a poorly functioning heat exchanger. Since the only added cost to the precooler is the additional pumping power required to overcoming a larger pressure drop, even a poorly functioning precooler may have added net benefit.

4 Reverse-Brayton cryogenic refrigeration

A potential type of cryogenic refrigeration cycle that may be incorporated is a reverse-Brayton refrigeration cycle. An analysis is conducted to determine the best-case compressor energy consumption rates for a cryogenic reverse-Brayton refrigeration cycle which is shown in Fig. 2. In a reverse-Brayton refrigeration cycle the working fluid circulates between components as a gas in a closed loop without changing phase. To capitalize on existing cryogenic cooler technology, the most likely working fluid is helium. Heat is removed from the cold reservoir in a reverse-Brayton refrigeration cycle and rejected to a warmer environment. In this case, the cold reservoir T_C is the temperature requirement of the CO_2 deposition chamber, which is the temperature required to desublimate the CO_2 (T_i). The hot temperature T_H is the ambient environmental temperature depending upon location. The energy $\dot{Q}_{1-2}$ is the energy removed

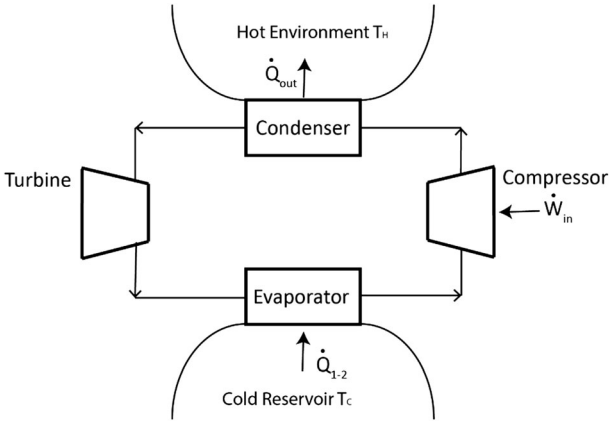

Fig. 2 Schematic diagram of a cryogenic reverse-Brayton refrigeration cycle

from the CO_2 deposition chamber while $\dot{Q}_{out}$ is the heat rejected to the environment. The work of the compressor is $\dot{W}_{in}$.

The coefficient of performance (COP) of a refrigeration cycle is defined as

$$\beta = \frac{\dot{Q}_{1-2}/\dot{m}_{ref}}{\dot{W}_{in}/\dot{m}_{ref}} = \frac{Q_{1-2}}{W_{in}} \tag{18}$$

No system can perform better than the Carnot COP

$$\beta_{Carnot} = \frac{T_C}{T_H - T_C} \tag{19}$$

The Carnot COP is a theoretical maximum for the best-possible performing cryogenic refrigeration system. More realistically, systems perform at COP which is a percentage of the Carnot COP (efficiency) as defined below

$$\eta = \frac{\beta}{\beta_{Carnot}} \tag{20}$$

Typically, the maximum efficiency of cryogenic refrigeration systems is around 0.15 (Radenbaugh 2004), though significantly better values may be achievable with research.

5 Results and discussion

All work required to desublimate CO_2 is reported using a cryogenic COP efficiency, $\eta = 0.15$. In order to investigate the effect of temperature, Figure 3 plots the work required to desublimate CO_2 as a function of ω with no precooler for the various ambient temperatures. Results here are reported both on a per-mass-air (Fig. 3(a)) and a per-mass-CO_2 desublimated (Fig. 3(b)) basis. In the CO_2 desublimation literature, it is customary to report results on a per-mass-CO_2 desublimated basis; however, reporting results on a per-mass-air basis also provides insight. Furthermore, example parameters used in the calculations for the optimal case with no fouling ($T_{ambient,\ in} = -90\,^{\circ}\mathrm{C}$, $\omega = 0.8$, $\epsilon = 0.7$) are provided in Table 2.

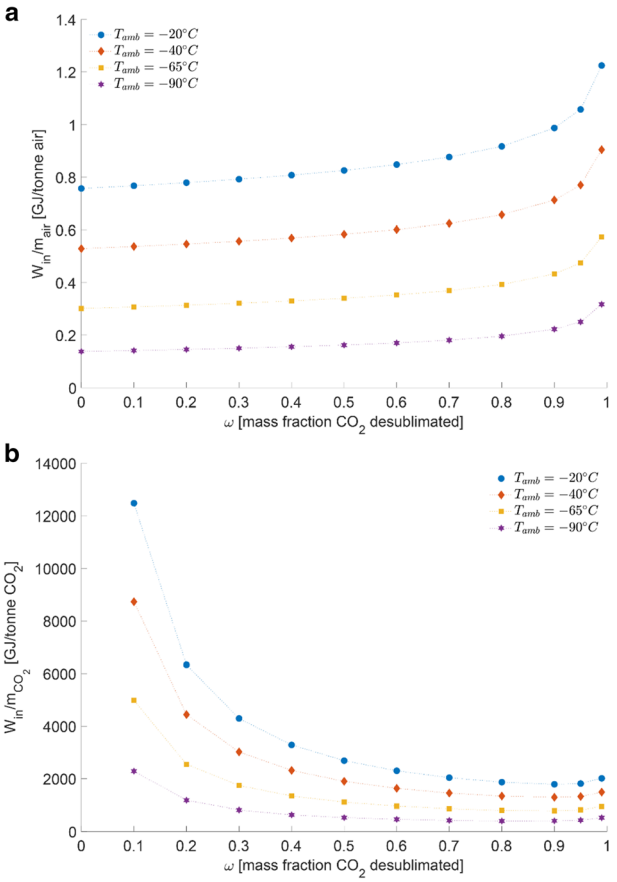

Fig. 3 Compressor input work required to desublimate CO_2 in deposition chamber at various ambient temperatures without precooler for η = 0.15. Results show (a) Energy per mass air flowing through desublimation chamber, and (b) Energy per mass CO_2 desublimated

According to Fig. 3(a), as the target amount of CO_2 to be desublimated increases, the target desublimator temperature decreases. In order to cool a unit mass of air to lower temperatures, the required cryocooler energy input must increase. Further, at lower values of ω, the energy requirements increase slowly with increasing ω. For higher values, of ω, particularly once ω becomes greater than 0.8, the energy requirements increase more rapidly with increasing ω, this is due to the exponentially decreasing desublimation temperature as ω approaches unity.

Table 2 Example parameters used in the thermodynamic analysis of the optimal CO_2 desublimation case with no fouling ($T_{ambient,\ in} = -90$ ° C, $\omega = 0.8, \epsilon = 0.7$)

$T_{ambient,\ in}$ [°C]	-90.00	h_{ig} · [kJ/kg]	624.64		
T_{out} [°C]	-107.89				
State 1		State 2		State i	
$\dot{m}_{CO_2,\ 1}$ [kg/s]	0.00061525	$\dot{m}_{CO_2,\ 2}$ [kg/s]	0.00012305	$\dot{m}_{CO_2,\ i}$ [kg/s]	0.00049220
$\dot{m}_{a,1}$ [kg/s]	1	$\dot{m}_{a,2}$ [kg/s]	1		
$P_{CO_2,\ 1}$ [*atm*]	0.00040500	$P_{CO_2,\ 2}$ [*atm*]	0.000080999		
T_1 [°C]	-131.73	T_2 [°C]	-149.62		

Figure 3(b) shows the energy required to desublimate CO_2 on a per-mass-CO_2 basis. This figure shows the optimum mass fraction target of CO_2 to be desublimated. At lower target mass fractions, energy is wasted cooling down the air to lower temperatures without much CO_2 desublimated. However, at very high target mass fractions, it takes increasingly lower temperatures to desublimate increasingly smaller amounts of CO_2. Therefore, an optimal target mass fraction is observed where the compressor work required per unit mass CO_2 desublimated is minimal. This point occurs when $\omega \sim 0.9$ for ambient temperatures equal to or less than -65 °C and $\omega \sim 0.8$ for T_{amb} = -90 °C. Figures 3(a) and 3(b) also demonstrate that for a given value of ω, a decrease in T_{amb} yields a roughly commensurate decrease in the energy required to drive the system, which in turn drives the siting to cold arctic environments.

Figure 4 shows the compressor work energy required to desublimate mass fraction ω of CO_2 where T_{amb} = -90 °C assuming a COP efficiency of 0.15 of Carnot. Results here are reported both on a per mass air (Fig. 4(a)) and a per mass CO_2 desublimated (Fig. 4(b)) basis. Results compare the effect of the precooler effectiveness on performance. It can be noticed that in both of the charts, for ϵ = 0.9 and 0.95, the trend line stops at ω = 0.6 and 0.4, respectively.

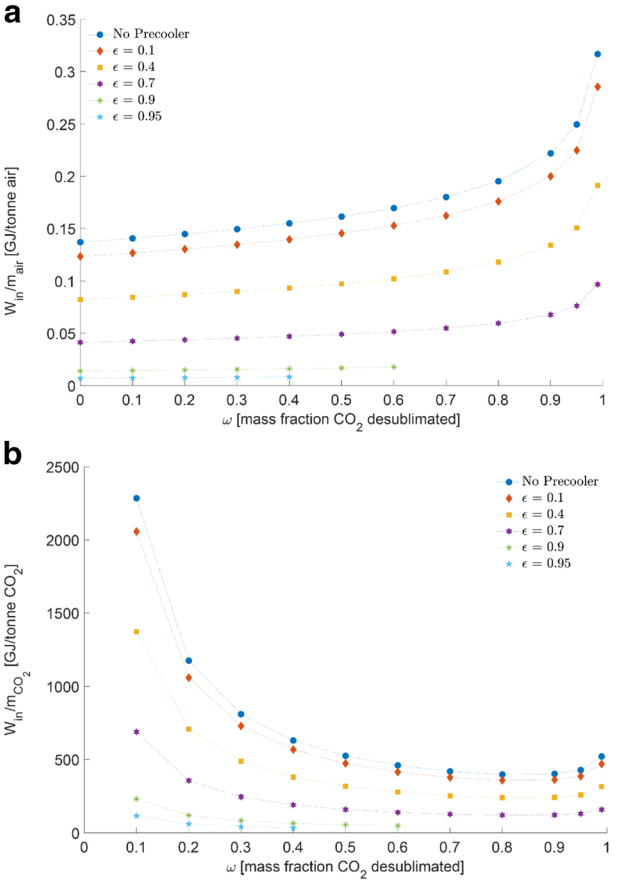

Fig. 4 Compressor input work required to desublimate CO_2 in deposition chamber with added precooler for T_{amb} = -90 °C for η = 0.15. Results show (a) Energy per mass air flowing through desublimation chamber, and (b) Energy per mass CO_2 desublimated

This is because a precooler with an effectiveness of 0.9 or 0.95 will cool the inlet air to below the CO_2 desublimation point when the target ω becomes greater than 0.6 and 0.4, respectively. If the inlet air temperature is below the CO_2 desublimation temperature, then the CO_2 will start to desublimate in the precooler, fouling the heat exchanger (Yu et al. 2017). The premature desublimation and fouling create complications beyond the scope of the current study and therefore candidate designs for this heat exchanger will be developed in a future study.

The optimal mass fraction to minimize compressor work per unit mass CO_2 desublimated (See Fig. 5) occurs at $\omega = 0.8$ for no precooler and for $\epsilon = 0.1$, 0.4, and 0.7. It occurs at $\omega = 0.6$ and 0.4 for $\epsilon = 0.9$ and 0.95, respectively. For the optimal case when no precooler is present, the compressor work to desublimate $\omega = 0.8$ CO_2 is 396 GJ/tonne CO_2. When a precooler is present which has an effectiveness of 0.95, the compressor work for $\omega = 0.4$ is equal to 33 GJ/tonne CO_2. As seen by the numbers, adding a precooler with very high effectiveness can reduce the compressor work by nearly 92%.

These results extend the analysis presented by von Hippel (2018), who examined the $\omega = 0.9$ cases only. In that paper, the output environmental temperature of the refrigeration system was erroneously set to the exit temperature of the desublimator heat exchanger rather than the

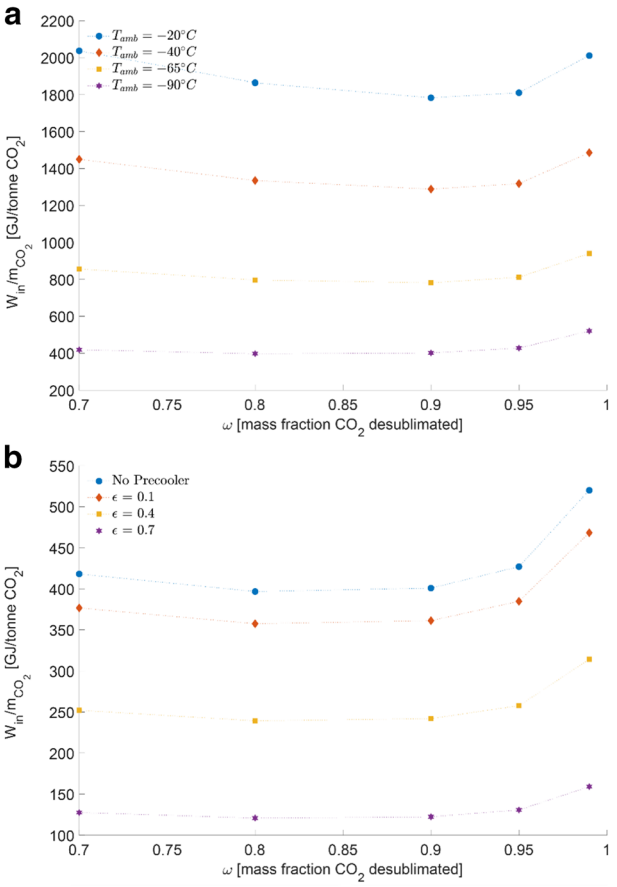

Fig. 5 Zoomed-in diagram showing minimum W_{in} per CO_2 desublimated for $\omega \geq 0.7$ for (a) Figure 3(b) and (b) Figure 4(b)

ambient temperature, making the previously published values too low. Calculations from von Hippel (2018) were rerun using the ambient temperature as the hot environmental temperature and 15% Carnot efficiency. In the current investigation, for T_{amb} = -20 °C, $\omega = 0.9$, and $\epsilon = 0.9$, the calculated work is 184 GJ/tonne CO_2, and the approach of von Hippel (2018) yields a corrected value of 174 GJ/tonne CO_2. Further, for T_{amb} = -40 °C, $\omega = 0.9$, and $\epsilon = 0.9$ the work is calculated as 133 GJ/tonne CO_2 and the von Hippel (2018) approach yields a corrected value of 126 GJ/tonne CO_2, showing congruency between the two simulations.

6 Concluding remarks

The techniques of psychrometrics were used to model air-CO_2 mixtures at the gas-to-solid phase boundary of CO_2 in order to model a direct-air capture CO_2 system. The model included a thermodynamic cryocooler and a precooler with a varying mass fraction of desublimated CO_2, all in cold Arctic/Antarctic regions where the proposed system might be operated. This analysis finds that the optimal CO_2 removal fraction to minimize energy input per unit mass of CO_2 occurs in the vicinity of $\omega = 0.8$ to 0.9, except for precooler effectiveness $\epsilon \geq 0.7$, where CO_2 begins to solidify inside the precooler before reaching the cryocooler. This phenomenon fouls the precooler, negating its effectiveness. For very high values of precooler effectiveness, compressor work can be $\leq$ 50 GJ/tonne CO_2. This value is substantially above the energy required to operate chemical-based direct air capture, which has been estimated at 1.20 to 1.73 GJ/tonne (Stolaroff et al. 2008), 7.96 GJ/tonne (Zeman 2007), and 5.0 to 9.9 GJ/tonne (Realmonte et al. 2019). Yet, substantial efficiency improvements and system enhancements could drive down the above 50 GJ/tonne value, making it competitive with these approaches. Additionally, the cost and scalability of each approach may not directly scale with the input energy costs, particularly in locations with steady and strong winds (Parish and Bromwich 1987; Agee et al. 2013).

Further system efficiencies could be realized via a precooler designed to capture solidified CO_2 and eliminate fouling as well as advances in the COP for cryogenic systems. Subsequent research should also include approaches that could drive down the energy cost for desublimating CO_2 by increasing T_{desub} (e.g., (Ehre et al. 2010)), enhancing radiative cooling (Chen et al. 2016) to both lower the effective ambient temperature and the refrigerator hot-side temperature, and preconcentrating CO_2.

References

Agee E, Orton A, Rogers J (2013) CO_2 snow deposition in Antarctica to curtail anthropenic global warming. J App Meteor & Climat 52:281–288

Agee E, Orton A (2016) An initial laboratory prototype experiment for sequestration of atmospheric CO_2. J Appl Meteor & Climat 55:1763–1770

Baxter L, Baxter A, Burt S (2009) Cryogenic CO2 capture as a cost-effective CO2 capture process. International Pittsburgh Coal Conference, Pittsburgh, PA. Available from: sesinnovation.com/news/documents/cccpittsburghcoalconference.pdf (Accessed 15/05/2017).

Chen Z, Zhu L, Raman A, Fan S (2016) Radiative cooling to deep sub-freezing temperatures through a 24-h day-night cycle. Nat Commun 7:13729

Ehre D, Lavert E, Lahav M, Lubomirsky I (2010) Water freezes differently on positively and negatively charged surfaces of pyroelectric materials. Science 327:672–667

Hansen J, Sato M, Kharecha P, Beerling D, Berner R, Masson-Delmotte V, Pagani M, Raymo M, Royer DL, Zachos JC (2008) Target atmospheric CO2 : Where should humanity aim? Open Atmos Sci J 2:217–231
IPCC (2018) Global warming of 1.5 °C, URL: http://www.ipcc.ch/report/sr15/ last accessed 10/1/2019
Keith D, Ha-Duong M, Stolaroff J (2006) Climate strategy with CO_2 capture from the air. Climatic Change 74: 17–45
Lackner KS, Brennan S, Matter JM, Park AHA, Wright A, van der Zwaan B (2012) The urgency of development of CO2 capture from ambient air. Proc Natl Acad Sci 109:13156–13162
Lemmon E, Jacobsen R, Penoncello S, Friend D (2000) Thermodynamic properties of air and mixtures of nitrogen, argon, oxygen from 60 to 2000 K at pressures to 2000 MPa. Journal of Physical and Chemical Reference Data 29
Lemmon EW, Bell I, Huber ML, McLinden MO (2018) NIST Standard Reference Database 23: Reference Fluid, Thermodynamic, and Transport Properties-REFPROP, Version 10.0, National Institutes of Standards and Technology
Marty C, Philipona R, Delamere J, Dutton EG, Michalsky J, Stamnes K, Storvold R, Stoffel T, Clough SA, Mlawer EJ (2003) Downward longwave irradiance uncertainty under arctic atmospheres: Measurements and modeling. J Geophys Res 108:4358–4370
Moran MJ, Shapiro HN, Boettner DD, Bailey MB (2018) Fundamentals of engineering thermodynamics, ninth ed. Wiley, Hoboken NJ USA
Parish TR, Bromwich DH (1987) The surface windfield over the Antarctic ice sheets. Nature 328:5154
Petty GW (2008) A first course in atmospheric radiation, second edn. Sundog Publishing, Madison WI USA
Radenbaugh R (2004) Refrigeration for superconductors. Proceedings of the IEEE 1719-1734
Realmonte G, Drouet L, Gambhir A, Glynn J, Hawkes A, Köberle AC, Tavoni M (2019) An inter-model assessment of the role of direct air capture in deep mitigation pathways. Nat Commun 10:3277
Span R, Wagner W (1996) A new equation of state for carbon dioxide covering the fluid region from the triple-point temperature to 1100 K at pressures up to 800 MPa. J Phys Chem Reference Data 25
Stolaroff JK, Keith DW, Lowry GV (2008) Carbon dioxide capture from atmospheric air using sodium hydroxide spray. Environ Sci Technol 42:2728–2735
von Hippel T (2018) Thermal removal of carbon dioxide from the atmosphere: Energy requirements and scaling issues. Climatic Change 148:491–501
Walden VP, Warren SG, Murcray FJ (1998) Measurements of the downward longwave radiation spectrum over the Antarctic plateau and comparison with a line-by-line radiative transfer model for clear skies. J Geophys Res 103:3825–3846
Yu Z, Miller F, Pfotenhauer J (2017) Numerical modeling and analytical modeling of cryogenic carbon capture in de-sublimating heat exchanger. IOP Conference Series: Materials Science and Engineering 278
Zeman F (2007) Energy and Material Balance of CO_2 capture from ambient air. Environ Sci Technol 41:7558–7563

Affiliations

Sandra K. S. Boetcher[1] · **Matthew J. Traum**[2] · **Ted von Hippel**[3]

[1] Mechanical Engineering, Embry-Riddle Aeronautical University, Daytona Beach, FL, USA

[2] Mechanical and Aerospace Engineering, University of Florida, Gainesville, FL, USA

[3] Physical Sciences, Embry-Riddle Aeronautical University, Daytona Beach, FL, USA